Modeling of the Section Capacitance to Interface with a S3R

A. Fernández, J.R. González

European Space Agency, Keplerlaan 1, 2201AZ Noordwijk, The Netherlands,
Email: Arturo.Fernandez@esa.int

ABSTRACT
Cell capacitance is a well-known parameter in silicon solar cells. Its effects on the power units, specially on the S3R, is also well known since it has to be taken into account to design them. The capacitor energy is discharged into the power switch and the dissipation increases. Moreover, it introduces a delay in the energy transfer from the array to the main power bus. In triple junction solar cells, this parasitic element becomes far more complex and is not so well characterized. This paper addresses this issue and proposes a large signal model to be used in combination with a S3R.

1. INTRODUCTION

Junction capacitance is a well-known issue in silicon semiconductors. There are two main contributors to this parasitic effect:
-The depletion layer (or transition) capacitance
-The diffusion capacitance
The first one is very simple to explain because it has the same concept as a conventional capacitor: two metal plates separated by a dielectric material. In the case of a semiconductor junction (e.g in a silicon diode), the depletion layer between the n- and p-sides of a p–n-diode serves as an insulating region that separates the two diode contacts. Thus, the diode in reverse bias exhibits a depletion-layer capacitance, also known as junction capacitance. This concept is shown in Fig. 1.

In reverse bias the width of the depletion layer depends on the bias voltage. In fact, the layer is widened with increasing reverse voltage bias v_R, and the capacitance is accordingly decreased. In a simplified model, the junction capacitance is:

$$C_j = k\varepsilon_0 \frac{A}{w(v_R)} \quad (1)$$

with A being the device area, κ the relative semiconductor dielectric permittivity, ε_0 the electric constant, and w the depletion width.

In forward bias, besides the above depletion-layer capacitance, minority carrier charge injection and diffusion occurs. A diffusion capacitance exists expressing the change in minority carrier charge that occurs with a change in forward bias as shown in Fig. 2. In terms of the stored minority carrier charge, the diode current i_D is:

$$i_D = \frac{Q_D}{\tau_T} \quad (2)$$

where Q_D is the charge associated with diffusion of minority carriers, and τ_T is the transit time, the time taken for the minority charge to transit the injection region. Typical values for transit time are 0.1–100 ns. On this basis, the diffusion capacitance is calculated to be:

$$C_D = \frac{dQ_D}{dv_D} = \tau_T \frac{di_D}{dv_D} = \frac{i_D \cdot \tau_T}{V_{th}} \quad (3)$$

Generally speaking, for usual current levels in forward bias, this capacitance far exceeds the depletion-layer capacitance.

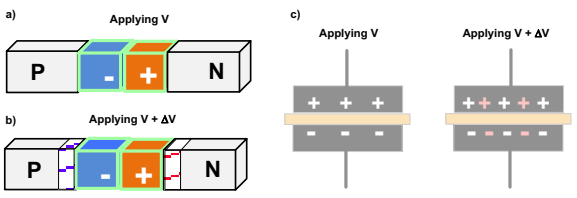

Fig. 1: a) diode with a depletion layer between two conductive blocks; b) The effect of the bias voltage on the depletion layer is shown; c) equivalent effect on a capacitor

2. STATIC TRIPLE JUNCTION CELL CAPACITANCE

Starting from the previous basis, the authors in [3] presented a multi junction solar cell capacitance model. The concept relies on modelling the capacitance of the individual cells one by one and then building the full model connecting all of them in series.

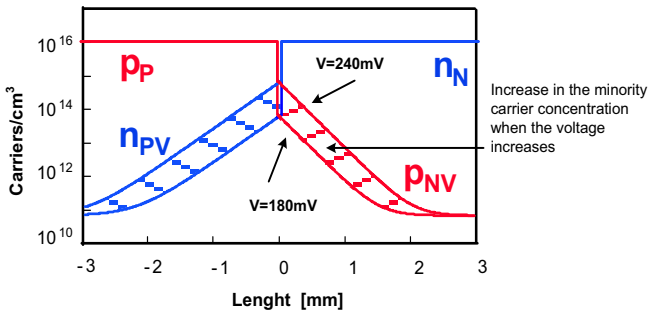

Fig. 2: diffusion capacitance effect due to the increase in the minority carrier concentration when the bias voltage increases

The three junctions have different electrical characteristics (I_F, V_F) and different capacitance values. Moreover, this junction capacitance is voltage dependent as was shown before. Thus, the full model is quite complex and the prediction of the behavior of the full stack is not obvious.

Fig. 3a shows a simplified model of the three junctions in series, each one with its own voltage dependent capacitor in parallel. Fig. 3b shows the capacitance value of the three junctions as a function of voltage. The top cell is the GaInP cell, the middle one is the GaInAs cell and the bottom one is the Ge cell. The basic characteristics are shown in Table 1. The values used in the model are based on the values obtained in [3].

When the power system topology is based on a S3R, the solar array sections will be subject to a large signal excursion since there are two possible states:

- shunted or
- biased to the bus voltage level.

As a consequence, each cell will be subject to an equivalent excursion from zero to a corresponding voltage level (typically close to the Maximum Power Point (MPP) value). The effects of this transient at cell level are not as simple as one would have thought as

TABLE1.: BASIC CELL PARAMETERS OF THE AZUR TRIPLE JUNCTION SOLAR CELL

Cell	V_F [V]	I_F [A]	C_0 [µF]
GaInP	1.41	0.502	2.47
GaInAs	1.021	0.535	1.28
Ge	0.253	0.881	3.92

will be explained in the following paragraphs. To simplify the explanation and to make the test generic, we will assume that the cell excursion will go from zero to open circuit voltage V_{OC}.

3. CELL DYNAMIC CHARGE

When the S3R is shunting the section and, as a consequence, the solar cells, the first assumption could be that the three junctions are short-circuited and that the three cell capacitors have no charge. However, the real situation is totally different. Due to the fact that each subcell (junction) has a different IV characteristic, and the fact that the three subcells are connected in a monolithic series association, the total stack current is limited by the one with the smallest current value. In our case, the GaInP subcell. The main outcome of this very particular configuration is that the electrical equilibrium of the stack is such that the top subcell is reverse biased but the other two are forward biased to its saturation levels (1.0 V and 0.2 V respectively). Thus, the top subcell voltage level will be -1.2 V, so that the total voltage of the series association is zero, consistent with the short circuit condition .

The main consequence of this situation is that, when the short circuit is released, the middle and the bottom subcells are already fully charged. Hence, they will not undergo any sort of transient. Only the top subcell

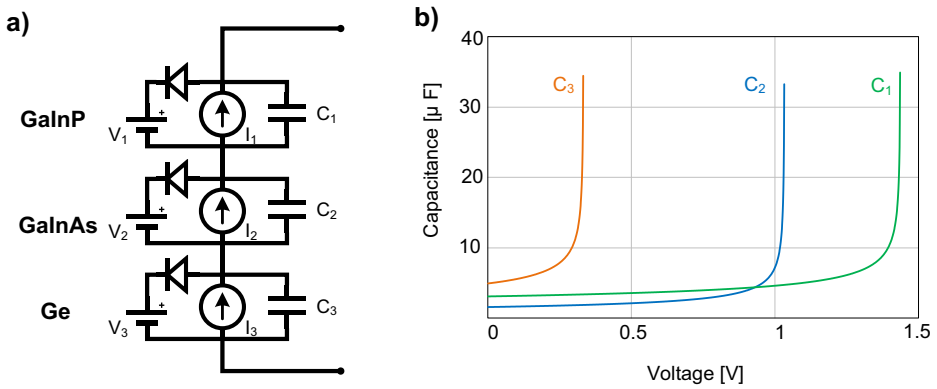

Fig. 3: a) simplified model of a triple junction solar cell; b) capacitance value as a function of voltage for the three sub-cells.

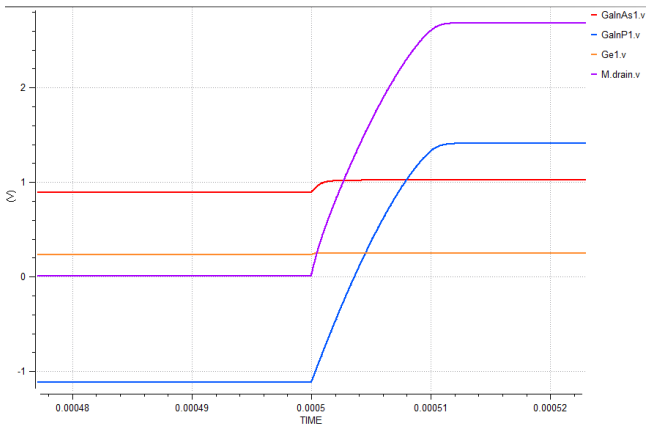

Fig. 4: release transient in a triple junction solar cell. Red: GaInAs, Orange: Ge, Blue: GaInP, Purple: Total cell voltage

(GaInP) will be subject to a voltage excursion from the reverse biased situation (-1.2 V) to the final open circuit situation (+1.4 V). Fig. 4 shows the voltage values on the three cells when the short-circuit is released. The very important conclusion of this is that, during this transient, the dynamic behavior is only influenced by the GaInP subcell.

To obtain a large signal model of this dynamic behavior, we need to model an equivalent capacitor that will be placed in parallel with the full three subcell stack, not only across one sub-cell. Moreover, the voltage excursion to which it will be subject is also going to be different. In the case of the GaInP subcell, it goes from -1.2 V to +1.4 V while in the full cell model it goes from 0 V to + 2.6V. Moreover, as was explained above, the capacitance is voltage dependent.

As was explained in [4], to model this case we need to consider the equivalent electrical charge that is loaded in the capacitor. Hence, the charge equivalent linear capacitance is:

$$C_{eq,Q} = \frac{1}{V_A}\int_0^{V_A} C_x(v_C)dv_C \qquad (4)$$

which will have the same amount of stored charge at V_A as the nonlinear capacitor C_x. As seen from (4), this value is simply the average of the C_x curve with respect to voltage.

In the case of the GaInP subcell, this average value is 2.25 µF. Fig. 5 shows a simulation where both the nonlinear model and the charge average capacitor model are released from short-circuit. As can be seen, they both reach the open circuit status at the same time. The transient shape is not identical since the simplified model is a conventional capacitor and the transient shape is a simple straight line.

However, note that in fact, the transient time is the actual figure that is important for the S3R control loop design. This value has to be taken into account to avoid double section switching. Neither the shape nor the energy are relevant in this case.

4. Cell Dynamic Discharge

The transient going from V_{OC} to zero is completely different though. In this case, the three junctions are in an open circuit state and hence, their capacitors are fully charged. When the cell is short-circuited, all this energy is extracted from the 3-subcell stack and transferred to the switching element which is the S3R MOSFET.
During the transient, the three junctions are actually discharged and undergo a transient from V_{OC} to zero as shown in Fig. 6a. At this point, the transient is finished for an external viewer (as seen in the purple trace). This means that no more energy is extracted and that the voltage stack will not move any more once it has reached zero volts.

However, internally in the cell the action has not finished. The internally generated photocurrent will continue charging the elements and the transient at individual subcell level continues. The final status will be as explained in the paragraph above: the top subcell will be reversed biased while the middle and the bottom subcells will be forward biased again. Fig, 6b shows this full transient.

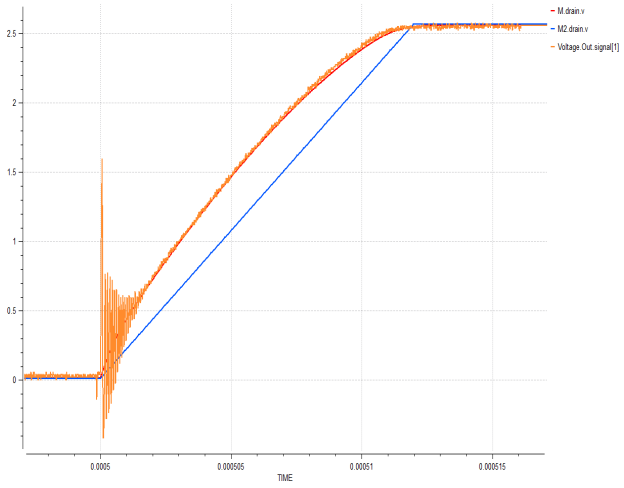

Fig. 5: simulation of the release transient in a triple junction solar cell. Blue: simplified average model, Red: non-linear model, Orange: test results.

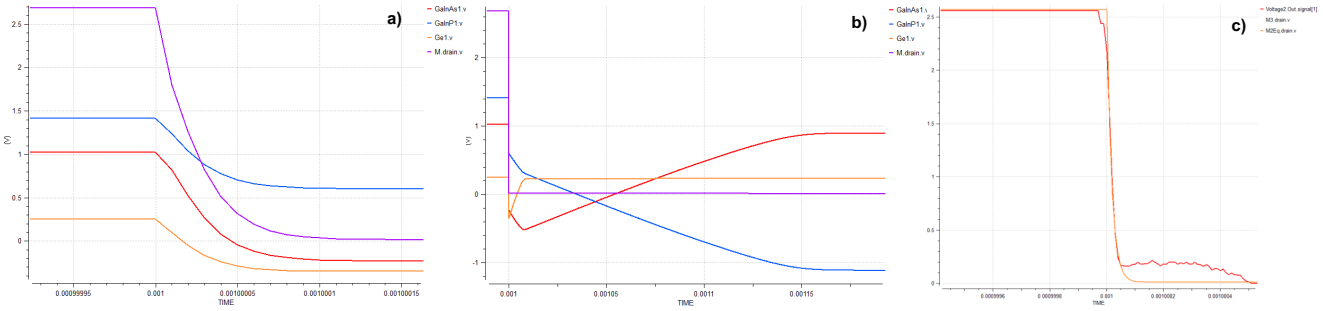

Fig. 6: a) first part of the energy discharge transient; b) full transient of the energy discharge in a triple junction solar cell. Red: GaInAs, Orange: Ge, Blue: GaInP, Purple: Total cell voltage; c) simplified model (orange) compared to the test result (red).

In terms of large signal modeling at cell level, the key point is to model the energy that has been transferred to the switch. In this case, the calculation has to be done in a different way.

The total energy in a nonlinear capacitor is given by integrating the product of C_x and v_c across the voltage range e.g. from 0 to V_{OC} [5].

$$E_C = \int_0^{V_A} v_C C_x(v_C) dv_C \tag{5}$$

This energy can then be used to find a linear capacitance value that contains the same amount of energy at V_A by considering the solution to the energy stored in some equivalent capacitor C_{eqE}, which is linear, constant-valued:

$$E_C = \frac{1}{2} C_{eq,E} V_A^2 \tag{6}$$

By combining (3) and (4) an expression for the energy -equivalent linear capacitor can be obtained:

$$C_{eq,E} = \frac{2}{V_A^2} \int_0^{V_A} v_C C_x(v_C) dv_C \tag{7}$$

where C_{eqE} and C_x store the same amount of energy at $v_c = V_A$.

In the case of the triple junction solar cell, this calculation has to be performed individually for the three subcells. Then, the equivalent capacitor has to be calculated in such a way that its stored energy is the same as the sum of the three individual energies. In the case of the AZUR 3G28 cell, this value is 840 nF. Fig. 6c shows the comparison between a simplified model with a linear capacitor (840 nF) and the test results with that cell on the continuous light sun simulator.

As can be seen, this value is around 2.5 times smaller than the one calculated for the release transient.

It has to be noted that this value is needed for a completely different calculation in the S3R. The section that is switching will dissipate this energy and hence, the thermal interface has to be designed accordingly. The snubber used to soften the peak current on the MOSFET will be also affected by this value.

As can be seen, the model is asymmetric since the equivalent capacitance is different depending on the transition direction. Moreover, both values are needed for two very different design aspects of the S3R: the capacitor modeling the release transition is needed for the control loop design while the capacitor modeling the shunt transition is needed to design the thermal interface and the current snubber.

In terms of circuit modeling, it is now evident that the large signal behavior of a triple-junction solar cell cannot be replicated with a simple linear capacitor. The modeling is not complex though since it can be done with a capacitor which capacitance value changes depending on the current sense. When the capacitor is being charged, the value should be 2.25 µF while, when the capacitor is being discharged, the capacitance should be 840 nF.

5. String Modeling

Once the model of one individual cell has been obtained, the modeling of the full string can be tackled. One could be tempted to think that the string model is a simple series connection of single cells. However, this is not the case. In fact, what actually happens is very similar to what have been described for the triple junction subcell stack.
Fig. 7a shows a simplified model of a cell string. As can be seen, 4 cells are connected in series and each one of them has a bypass diode and a capacitor in parallel.

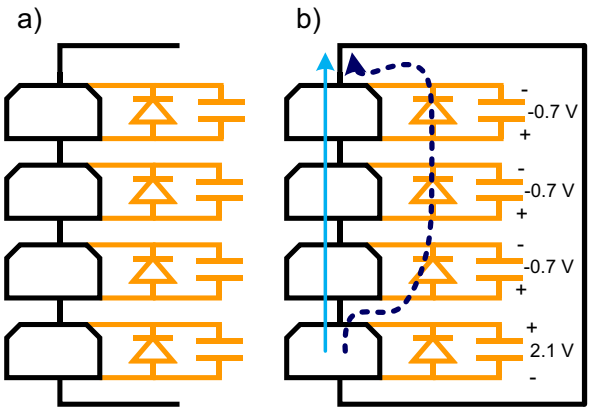

Fig. 7: a) 4 cells stack configuring a string. Each cell has a bypass diode and a capacitor in parallel; b) shortcircuited string with the excess current flowing through the bypass diodes.

In an ideal situation, all 4 cells would have exactly the same shortcircuit current. However, in reality each cell will have a slightly different current value. As a consequence, when the string is shunted it is electrically impossible that all four cells have zero volts and different current values flowing across them.
In the triple junction stack, the current value is limited by the subcell with the lowest current. In the string the situation is different because of the bypass diodes. The equilibrium condition will be that the cell with the highest current value will drive the string current and the excess with respect to other cells current will flow through the diodes.

The fact that the bypass diodes conduct the excess current has another important consequence: the cells in parallel with those diodes will be reverse biased.

Let's assume that the forward voltage drop of the bypass diode is V_D = 0.7 V and that the open circuit voltage of the solar cells is V_{OC} = 2.7 V. Under these constraints, the equilibrium condition to solve the shortcircuit will be as shown in Fig. 7b.
One cell is forward biased (+2.1 V) and three cells are reverse biased (-0.7 V). The cell in forward will adapt its voltage so that the overall stack has zero volts across it. In this case: 0.7 V x 3 = 2.1 V.

Coming back now to the capacitance, when the short circuit is released, the cell that is already forward biased will contribute very lightly to the transient. Its capacitance is already charged to 2.1 V and will have a negligible effect in the string transient as can be seen in Fig. 8a (blue trace).

At string level, the consequence is interesting: since one capacitance is already charged and does not contribute to the transient, the overall capacitance value will be equivalent to 3 capacitors in series instead of 4. Hence, the string capacitance will be C_{cell} / 3 and will be higher than in an ideal case where the 4 cells contribute to the transient. This can be clearly seen in Fig. 8b. The red trace shows the overall string voltage assuming that the four cells are shortcircuited while the blue trace shows a real 4 cell stack with 4 slightly different current values. As can be seen, the real case is slower than the ideal one: the equivalent string capacitance is C_{cell} / 3 instead of C_{cell} / 4.

Hence, to model a generic string we need to take into account the voltage drop across the bypass diodes (V_D) and the cell V_{OC} voltage. Depending on the ratio of those two voltages V_{OC} / V_D more or less cells' capacitances will need to be removed from the transient. In this example, the ratio is 2.7 / 0.7 = 3.85 so one out of every 4 cells will not contribute to the transient and the equivalent string capacitance will be increased accordingly.

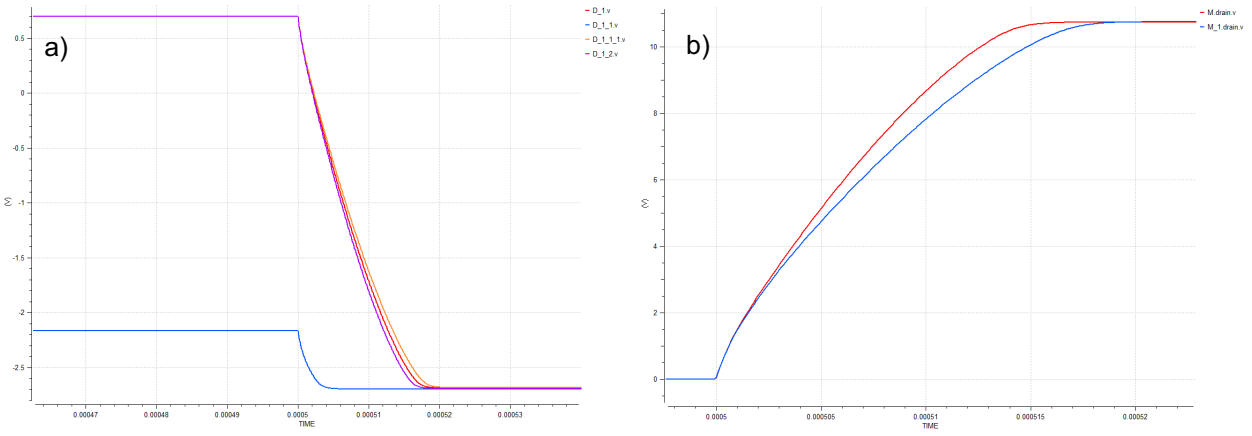

Fig. 8: a) voltage across the 4 cells of the string; b) overall string voltage; red trace: ideal string with 4 cells shortcircuited; blue trace: real string with 3 cells in reverse and 1 in forward.

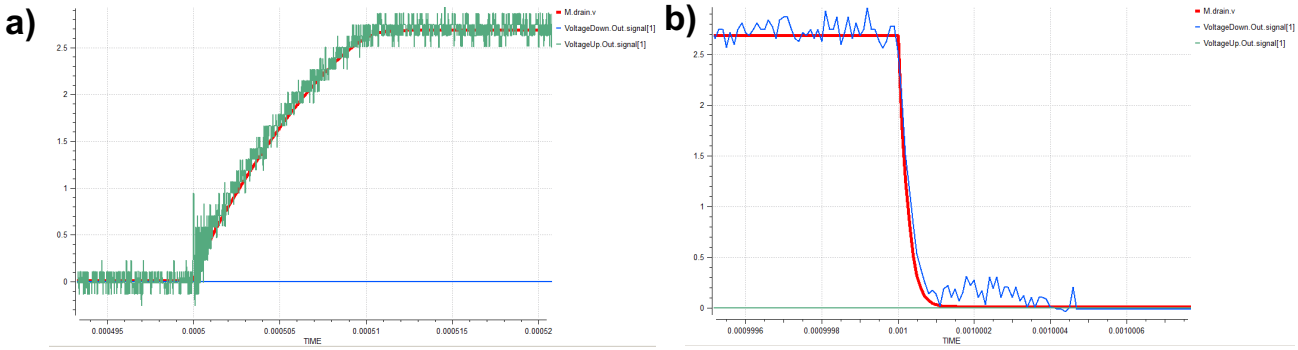

Fig. 9: a) Azur 3G28 release transient. Green: experimental result, Red: simulation result; b) shunt transient, Blue: experimental result, Red: simulation result.

6. Test Results

6.1 Continuous Light Sun Simulator

Several tests have been performed in order to verify this concept. A single cell has been placed in a temperature controlled holder and illuminated using continuous light under a triple source solar simulator. The initial calibration has been adjusted in such a way that the top sub-cell is the one limiting, as it is the case in real BOL conditions. A low r_{DSon} MOSFET has been placed in parallel with the cell and switched continuously at a frequency of 1kHz. The circuit arrangement has been carefully done to minimise the parasitic impedance and to have the cleanest possible switching.
The voltage between drain and source on the MOSFET was measured and compared to the simulation results. The model used in this case is the triple junction model with three separated nonlinear capacitors. Fig. 9a shows the release transient and Fig. 9b shows the shunt transient. In both cases, the model is able to mock the behavior of the real cell fairly well. As can be seen, the time scale is completely different.

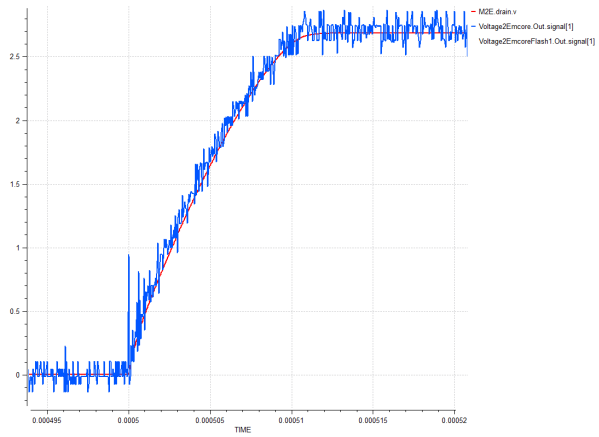

Fig. 10: Solaero cell release transient. Blue: experimental result; Red: simulation result with 3 non-linear capacitances model.

It takes a few µs to go from zero to V_{OC} while it only takes 100 ns to shunt the cell from V_{OC} to zero. Of course, this is due to the fact that both processes are completely different as has been explained in the previous paragraphs.

The same test was repeated for the Solaero ZTJ cell. The model was slightly tuned by adjusting the capacitance values. Solaero cells turned out to have around 15% lower capacitance. The result of the test compared to the simulation is shown in Fig. 10. As can be seen, both test and simulation results fit very well.

6.2 VLASS Continuous Flasher

Another set of testing has been done at the Airbus NL premises using a Vortek Large Area Solar Simulator (VLASS) [6] on an EM panel populated with Solaero ZTJ cells. In this case, the tests have been done at section level. In this case, the section had 46 cells in series and only 1 in parallel (46s1p).
The cell parameters have been adjusted accordingly with the outcome of the continuous light sun simulator and the results are shown in Fig. 11. The orange trace shows the release transient assuming that all 46 cells in series are initially shortcircuited. As can be seen, the experimental result is slower than the model. The red trace shows the model after adjusting the capacitance to take into account the effect of the string. In this case, the Solaero external bypass diode has a voltage drop of 0.8 V and the V_{OC} of the cell is 2.7 V. The ratio V_{OC} / V_D = 3.37, which means that out of every 4 cells, one will not contribute to the transient and 3 will undergo the full voltage swing from –0.8 V to 2.7 V. The adjustment implies an increase of the virtual capacitance of 33%. As can be seen, the simulated result adjust much better to the actual release test.

The shunt transient at panel level is more complicated than the release transient because of the transfer har-

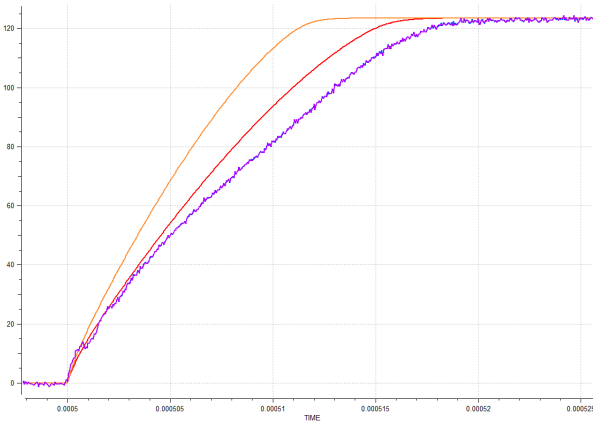

Fig. 11: section level (46s1p) release test with Solaero cells compared to the simulated results. Orange trace: ideal string; Red trace: model compensated with the string effect.

ness. The impedance between the section and the switch is much higher and has an important inductive component. Hence, unless it is very well characterized it is very difficult to match the simulation and the test results. Still, once the impedance value was adjusted, the result is also quite accurate.

6.3 ESTEC PASAN FLASHER

To continue investigating in the cell level and the section level modeling, the ESTEC Pasan flasher was also used to perform several tests. Moreover, in the Power Systems laboratory a model of the Herschel solar panel is available and hence, transient tests on a real SA section can be performed. This is very interesting since we could perform test both at cell and section level with the same light source. In this case, the flasher can provide a 14 ms light plateau that allows to visualize 14 full switching transients at 1 kHz.

However, instead of allowing the confirmation of the model, these test results have introduced some uncertainties that so far we have not been able to explain.

The results from these tests are significantly faster than the ones obtained from the other tests. Fig. 12a shows the comparison of a switching transient obtained on the same Azur 3G28 cell with the continuous light sun simulator (blue trace) and the Pasan flasher (orange trace). As can be seen, the latter is significantly faster than the first one. In fact, the equivalent capacitance is 3 times smaller.
Fig. 12b shows the same comparison but this time with the Solaero ZTJ cell. The situation is repeated here since the result from the Pasan Flasher (orange trace) is also faster than the continuous light sun simulator (blue trace).

The tests performed on the Herschel panel also show a transient result that is much faster than the one obtained with the model. Fig. 13 shows this comparison and, as can be seen, the flasher result is considerably faster than the model. In fact, to fit the model the capacitance should have been reduced by a factor of 3.

Furthermore, the test at cell level offer different relative speeds on the Azur and Solaero cells as shown in Fig. 14. When illuminated with the continuous light simulator, the Solaero cell (blue trace) is faster than the Azur (red trace) as shown in Fig. 14a. However, when illuminated with the Pasan flasher the results reverse as shown in Fig. 14b. The Azur cell (red trace) is faster than the Solaero cell (blue trace).

Note also that the results from the VLASS flasher shown in Fig. 11 are also slightly different from the results from the model calibrated with the continuous light even though, in this case, the test results are slower. Overall, it has not been possible to correlate results obtained with different light sources, even though all

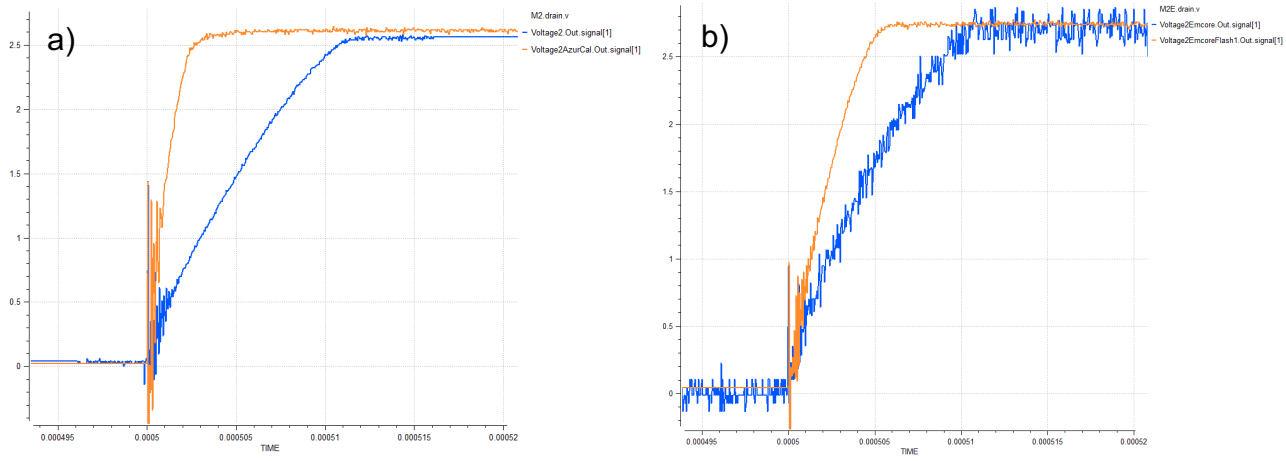

Fig. 12: a) Azur 3G28 release transient at cell level. Orange trace: Pasan flasher; Blue trace: continuous light simulator; b) Solaero release transient at cell level. Orange trace: Pasan flasher; Blue trace: continuous light simulator

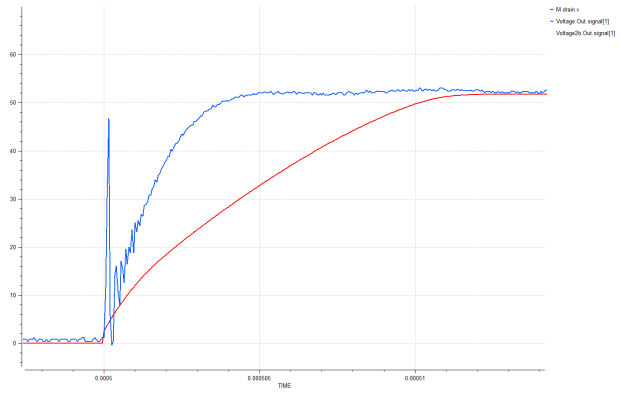

Fig. 13: Release test at section level (20s5p) on the Herschel panel. Blue trace: test result with the Pasan Flasher; Red trace: simulated result with the cell calibrated with the continuous light simulator.

of them are supposed to be calibrated to the AM0 spectrum. Or at least to provide results equivalent to those from AM0. A plausible explanation for these phenomena has not been found yet.

7. CONCLUSIONS

The cell capacitance on a triple junction solar cell is a complex parasitic effect to describe. Each one of the subcells has a nonlinear capacitance in parallel that is voltage dependent. The fact that each subcell has different electrical parameters implies that the release and the shunt transient are completely different. As a consequence, a simplified model has to account for this asymmetry and use different capacitance values for either transient. The main conclusion is that the equivalent release capacitor is around 2.5 times larger than the equivalent shunt capacitor. The paper shows how to calculate these simplified values and has demonstrated their validity by comparing test results from continuous light simulation with the model simulated results and showing a very good agreement. The slowing effect of the string arrangement has also been explained and validated in one test set-up.
However, the experiments with different light sources have given different results So far, it has not been possible to provide an explanation for those differences. Hence, there is still some work to be done in order to understand any possible influence of the test light source.

8. REFERENCES

[1] *John Sparkes (1994).* Semiconductor Devices *(2nd ed.). CRC Press.*

[2] Robert B. Darling (1995). A Full Dynamic Model for pn-Junction Diode Switching Transient. *IEEE Trans. Electron Devices*. vol. 42, no. 5, pp. 971-976

[3] Dynamic Modelling Of Multi Junction Gallium Arsenide Solar Arrays, N. Neugnot, X. Roy, R. Chouffot, M.E. Gueunier-Farret, J.P. Kleider, H. Barde, C. Baur, A. De Luca. ESPC??

[4] Circuit-Oriented Modeling of Nonlinear Device Capacitances in Switched Mode Power Converters, Daniel Costinett, Regan Zane, Dragan Maksimovic. APEC??

[5] R. W. Erickson and D. Maksimovi´c, Fundamentals of Power Electronics, Second Edition. New York, NY: Springer Science+ Business Media, LLc, 2001.

[6] T. Thrum, D. Camm, D. Parleniuk and D. Slootweg, "Characterizing state-of-the-art solar panels a new approach for large area testing," Photovoltaic Specialists Conference, 2000. Conference Record of the Twenty-Eighth IEEE, Anchorage, AK, 2000, pp. 1320 -1323. doi: 10.1109/PVSC.2000.916134

[7] Capacitance Measurements on Multi-Junction Solar cells, P. Rueda, E. Fernandez Lisbona, M. Diez Herrero, World Conference on Photovoltaic Energy Conversion, Poster 817.

[8] R. Blok, E. van den Berg, & D. Slootweg; Solar Cell Capacitance Measurement, ESPC 2002, p.597

[9] R. Anil Kumar, M. S. Suresh, and J. Nagaraju, Effect of Solar Array Capacitance on the Performance of Switching Shunt Voltage Regulator; IEEE Transactions on Power Electronics, Vol. 21, No. 2, March 2006 p.543

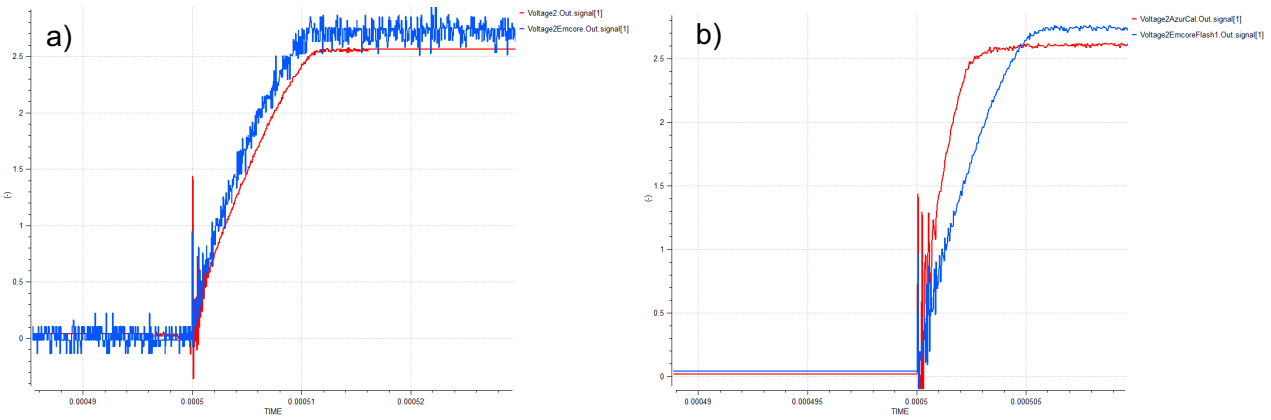

Fig. 14: comparison of the release transient between the Azur 3G28 (red trace) and the Solaero cell (blue trace). a) with the continuous light sun simulator; b) with the Pasan flasher.